ISBN: 978-3-95450-231-8 ISSN: 2673-5490 doi: 10.18429/JACoW-IPAC2023-TUPL017

WAKEFIELD ENERGY LOSSES IN THE UNDULATOR SECTION OF THE EUROPEAN XFEL

S. Tomin*, N. Lockmann, T. Wohlenberg, I. Zagorodnov
Deutsches Elektronen-Synchrotron DESY, Germany

Abstract

The energy loss of the electron beam due to synchrotron radiation and wakefields determines an undulator tapering in order to keep the resonance condition along the undulator. The contribution of synchrotron radiation to energy loss can be calculated analytically, whereas the calculation of wakefield energy loss requires knowledge of the beam current profile and the wakefield function at the undulator section. We present an experimental method for accurate measurement of the energy loss due to wakefields in the undulator section for the European XFEL. We compare the results of the measurements with earlier developed analytical model of the wakefunction.

INTRODUCTION

In the pre-saturation exponential growth regime, the electron beam's energy loss due to FEL interaction is much smaller than ρ - FEL scaling parameter. Thus, the energy exchange in this mode can be neglected, which allows us to use the uniform deflection parameter of the undulator K to maintain resonance. However, significant energy loss from spontaneous radiation emission, including higher harmonics (for $K > 1$), is occurring in long undulator beamlines, such as the European XFEL [1]. On the other hand, the undulator vacuum chamber contributes a significant portion to the wakefield impedance budget, which leads to beam energy losses that cannot be also neglected. To maintain the resonant condition in order to both not degrade the gain and maintain minimal SASE bandwidth [2], the undulator parameter K should be tapered as the beam energy decreases linearly with undulator distance.

The analytical formula for the energy loss of an electron beam in an undulator with length L and beam energy E due to spontaneous radiation is as follows:

$$U = \frac{4\pi^2}{3}\frac{r_e E^2 K^2 L}{mc^2 \lambda_w^2}, \quad (1)$$

where K is the undulator deflection parameter, λ_w the undulator period, r_e is classical radius of the electron. The contribution of the spontaneous radiation to the linear undulator taper can be easily calculated and it was included in the undulator control system from the beginning of the EuXFEL operation.

Calculation of beam energy losses due to wakefields requires not only knowledge of the wakefield impedance budget in the undulator beamline, but also of the electron beam current profile. An online non-invasive THz diagnostic CRISP [3] was installed at the European XFEL accelerator. The principle of operation is based on coherent diffraction radiation generated by an electron beam passing through an open aperture in the screen. The acquired THz spectrum of the electron beam is used in a reconstruction algorithm [4] to obtain the electron beam's current profile. Furthermore, an analytical model of the wakefunction for the undulator beamline has been established [5]. With these components available, the beam energy loss due to wakefields can be calculated, leaving the final step of verifying these findings through measurements.

EXPERIMENTAL SETUP

The European XFEL utilizes three long planar undulators: two hard X-ray undulators (SASE1/2) and one soft X-ray undulator (SASE3), Fig. 1. Each of these planar undulators consists of cells that adhere to a unified design. SASE1/2 contains 35 undulators with a period of 40 mm and SASE3 contains 21 undulators with a period of 68 mm. The individual cell contains a 5-meter long undulator and a 1.1-meter intersection, which houses components such as the quadrupole, phase shifter, BPM, and various vacuum components. The detailed description of the undulator vacuum chamber and its contribution to the wakefield impedance budget is listed in Ref. [5].

A simplified layout of the European XFEL facility is shown in Fig. 1. Wakefield energy losses were measured in the SASE3 undulator line because of the conveniently located diagnostics for electron beam energy measurements (for brevity we denote them by the beam energy monitor or BEM) and the relative simplicity of the vacuum chamber between the BEMs. As was mentioned in the Introduction, we used non-invasive CRISP THz diagnostics to measure the current profile.

Beam energy losses were measured for different current profiles. For this purpose, we varied the beam compression by scanning the Linac L1 chirp from -12 to +6 m^{-1} defined as $chirp = \frac{-kVsin(\phi)}{E_0+Vcos\phi}$, where V and ϕ are the voltage and phase of Linac L1, $E_0 = 130$ MeV is the initial energy of the beam before L1, and $k = 2\pi f/c, f = 1.3$ GHz. Details about the European XFEL three stage compression system and beam dynamics can be found in [6, 7]. The final beam compression was also independently controlled by the beam compression monitor (BCM), see Fig. 1.

Calibration of the Beam Energy Measurement Diagnostics

Beam energy monitors (BEMs) can measure the absolute energy of an electron beam with an accuracy of about 1%,

* sergey.tomin@desy.de

ISBN: 978-3-95450-231-8 ISSN: 2673-5490 doi: 10.18429/JACoW-IPAC2023-TUPL017

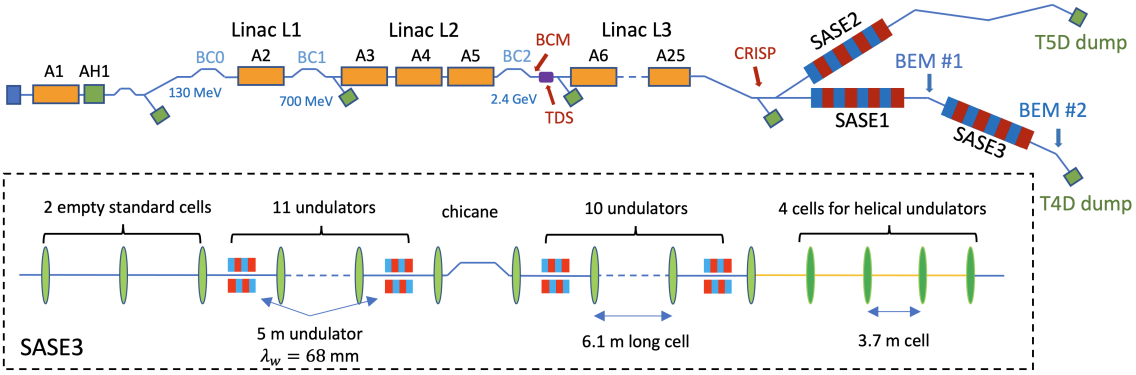

Figure 1: Simplified layout of the European XFEL facility.

which is not sufficient for direct measurement of beam energy changes in the 10-20 MeV range that are caused by wakefield energy losses. To overcome this limitation, we proposed a method for calibrating the BEM using spontaneous emission. As shown in Fig. 1, SASE3 consists of 215 m long undulators with a period of 68 mm. These undulators were sequentially closed in groups of three cells to a minimum gap corresponding to 660 eV at an beam energy of 14.1 GeV. The resulting beam energy changes were recorded by the BEM #2, as shown in Fig. 2. The theoretical prediction of Eq. (1) is also shown in the Fig. 2, and as you can see the measurements overestimate the real energy loss by a factor of $C = 1.28/1.99$. Similar techniques was used recently in Ref. [8] and shown good agreement with direct measurements.

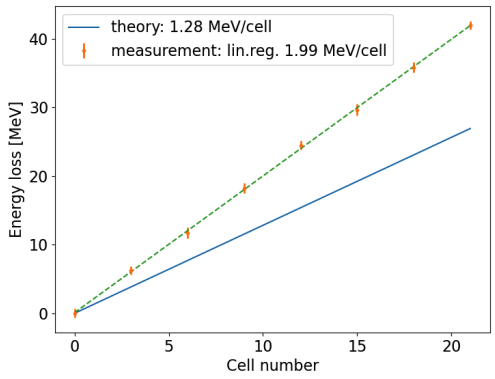

Figure 2: Measurements of the energy loss due to spontaneous radiation and linear regression of the measurement points. Blue line is energy losses according to theoretical prediction.

While performing the compression scan, it is reasonable to expect beam energy changes at the position of BEM #1, resulting from wakefields in the vacuum chamber of the accelerator segment from Linac L1 to BEM #1. Rather than applying the same calibration procedure to the first BEM, we maintained a constant beam energy throughout the entire experiment at this position, using energy FB based on the last RF station A25. This approach simplifies the experimental data analysis.

Wakefields Impedance Budget

Wakefield impedance budget or the vacuum section between two BEMs consists of three main parts: (1) 24 standard undulator cells, (2) 4 cells for the helical undulators and (3) round vacuum chamber of diameter 40.5 mm with length of 318 m. The standard undulator cell has length of 6.1 m and consists of the undulator elliptical pipe 5 m long and the intersection with length of 1.1 m. The details of the geometry are presented in [5], where an analytical form of the longitudinal wake function has been derived as well:

$$w_{\parallel}(s) = w_0(s) + \frac{\partial}{\partial s} w_1(s) + c\frac{R}{L}\delta(s), \tag{2}$$

$$w_0(s) = A\frac{Z_0 c}{\pi a^2} \exp\left(-\left(\frac{s}{s_0}\right)^{\alpha}\right) \cos\left(\frac{s}{s_1}\right), \tag{3}$$

$$w_1(s) = \frac{Z_0 c}{L\pi^2 a}\sqrt{2g_0 s}, \tag{4}$$

where $A = 0.937$, $a = 5$ mm, $\alpha = 1.29$, $s_0 = 33.8$ µm, $s_1 = 9.86$ µm, $g_0 = 123$ mm, $R = 30.5\,\Omega$. Some of coefficients are different from those published in Ref. [5] as we have corrected an error in the estimation of the wake of the round pipe in the intersection. To estimate the wake function for the helical cells we followed the same approach as in Ref. [5]. The length of the intersection is 0.7 m. At the moment of the experiment in March 2021 the undulator pipe of 3 m was yet not installed and presented by standard stainless steel pipe of large diameter of 40.5 mm.

In order to show relative contribution of these three main parts to the total wake we considered a short Gaussian bunch with rms length of 6 µm and charge of 250 pC. Figure 3 shows the wakes of the different parts. As expected the main contribution is done by the undulator cells.

RESULTS AND DISCUSSION

The experiment was conducted as follows. We scanned the Linac L1 chirp from +6 to -12 m^{-1}. Such a wide range was chosen to pass through the full compression. That is, initially, we had low compression and, accordingly, a low beam current amplitude at a positive chirp. As the chirp changed towards negative values, the compression increased, reaching its maximum at a chirp value of -8.5 m^{-1}. After passing

ISBN: 978-3-95450-231-8 ISSN: 2673-5490 doi: 10.18429/JACoW-IPAC2023-TUPL017

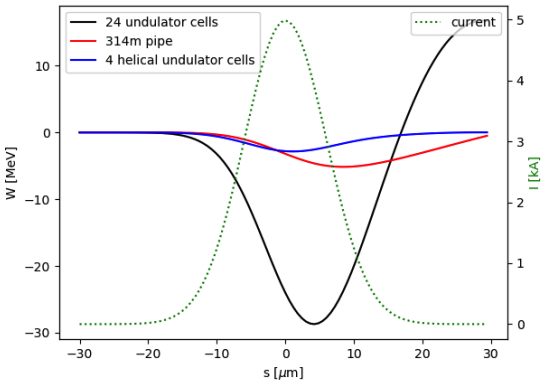

Figure 3: The wakes of different parts for the Gaussian bunch with length of 6 µm.

through full compression, the overcompression phase began, and the current amplitude started to decrease. The scanning step was chosen to be non-uniform, with a denser grid around the region of full compression. The scan was carried out twice, with the laser heater (LH) turned off and on. The laser heater introduces an uncorrelated energy spread, which results in a reduced current amplitude at full compression. The laser heater's intensity was selected to be near its maximum capacity, ensuring that its impact would be clearly visible. Consequently, we anticipated observing similar signals from the bunch compressor monitor (BCM) [9] but with distinct amplitudes. Lower signals correspond to the scan performed with the laser heater on, as depicted in Fig. 4. SASE3 undulators were opened to the maximum gap during wakefields energy loss measurement.

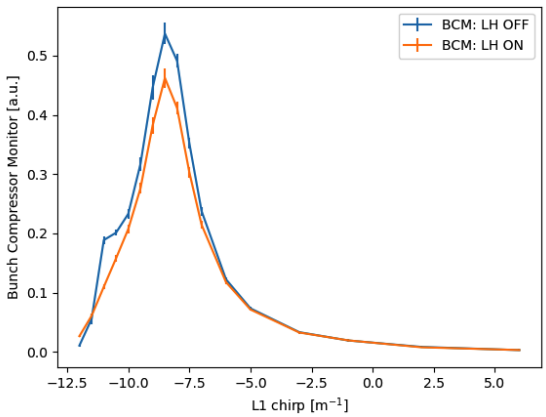

Figure 4: Signal from Bunch Compressor Monitor after the last bunch compressor BC2.

At each scanning step, we acquired the coherent diffraction radiation spectrum of the electron beam using CRISP for subsequent beam current profile reconstruction. In Fig. 5, several current profiles can be seen for different compression values and with the laser heater on and off.

Using the reconstructed current profile and knowing the wakefield impedance budget for the entire section, we calculated the electron beam losses due to wakefields. Direct measurement of the beam energy loss due to wakefields was carried out using BEM #2 and a previously measured cal-

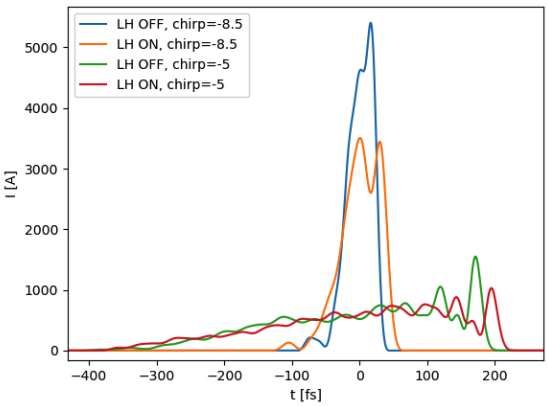

Figure 5: Reconstructed current profiles for full compression L1 chirp=-8.5 m^{-1} and lower compression L1 chirp=-5 m^{-1} with the laser heater off and on.

ibration coefficient $C = 1.28/1.99$. As mentioned earlier, the electron beam energy at the BEM #1 position remained constant due to energy feedback.

The direct measurement of beam energy loss is relative, as we assumed zero energy loss at the lowest compression (chirp = +6 m^{-1}). This assumption stems from the estimation that the current profile amplitude was order of 0.1 kA at the lowest compression point (chirp = +6 m^{-1}), corresponding to the wakefield energy losses on the order of 0.3-0.4 MeV. On the other hand, CRISP cannot provide reliable reconstructions for currents below 1 kA due to a low signal-to-noise ratio. Consequently, only a part of the scan can be utilized for the analytical estimation of wakefields energy losses, specifically for the Linac L1 chirp from -12 to -2.5 m^{-1}. The final result, as depicted in Fig. 6, demonstrates a good agreement between the analytical estimation based on CRISP reconstruction and direct measurements.

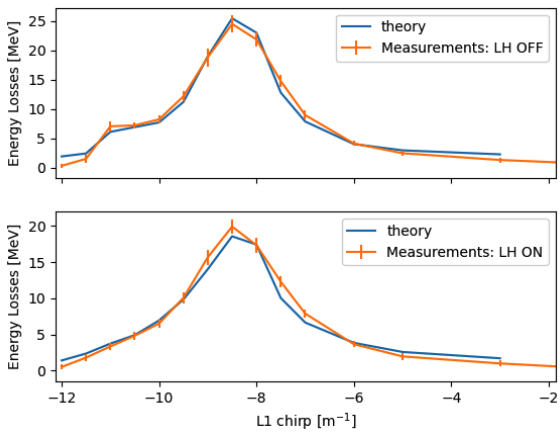

Figure 6: Beam energy loss due to wakefields in SASE3 undulator beamline. Comparison between direct measurements and analytical estimations.

REFERENCES

[1] W. Decking *et al.*, "A MHz-repetition-rate hard x-ray free-electron laser driven by a superconducting linear accelerator",

ISBN: 978-3-95450-231-8 ISSN: 2673-5490 doi: 10.18429/JACoW-IPAC2023-TUPL017

Nat. Photonics, vol. 14, p. 391, 2020. doi:10.1038/s41566-020-0607-z

[2] W. M. Fawley *et al.*, "Tapered undulators for SASE FELs", *Nucl. Instrum. Meth. Phys. Res. Sect. A*, vol. 483, pp. 537-541, 2002. doi:10.1016/S0168-9002(02)00377-7

[3] N. M. Lockmann, C. Gerth, B. Schmidt, and S. Wesch, "Non-invasive Thz Spectroscopy for bunch Current Profile Reconstructions at Mhz Repetition Rates", *Phys. Rev. Accel. Beams*, vol. 23, p. 112801, 2020. doi:10.1103/PhysRevAccelBeams.23.112801

[4] B. Schmidt, N. M. Lockmann, P. Schmüser, and S. Wesch, "Benchmarking Coherent radiation spectroscopy as a tool for high-resolution bunch shape reconstruction at free-electron lasers", *Phys. Rev. Accel. Beams*, vol. 23, p. 062801, 2020. doi:10.1103/PhysRevAccelBeams.23.062801

[5] I. Zagorodnov *et al.*, "Short-range longitudinal wake function of undulator lines at the European X-ray free electron laser", *Nucl. Instrum. Meth. Phys. Res. Sect. A*, vol. 1043, p. 167490, 2022. doi:10.1016/j.nima.2022.167490

[6] I. Zagorodnov and M. Dohlus, "A semi-analytical modelling of multistage bunch compression with collective effects", *Phys. Rev. Spec. Top. Accel. Beams*, vol. 14, p. 014403, 2011. doi:10.1103/PhysRevSTAB.14.014403

[7] I. Zagorodnov, M. Dohlus, and S. Tomin, "Accelerator beam dynamics at the European X-ray Free Electron Laser", *Phys. Rev. Accel. Beams*, vol. 22, p. 024401, 2019. doi:10.1103/PhysRevAccelBeams.22.024401

[8] S. Tomin, E. Schneidmiller, and W. Decking, "First measurement of energy diffusion in an electron beam due to quantum fluctuations in the undulator radiation", *Sci. Rep.*, vol. 13, p. 1605, 2023. doi:0.1038/s41598-023-28813-8

[9] C. Gerth and N. M. Lockmann, "Bunch Compression Monitor Based on Coherent Diffraction Radiation at European XFEL and FLASH", in *Proc. IBIC'21*, Pohang, Korea, Sep. 2021, pp. 400–403. doi:10.18429/JACoW-IBIC2021-WEPP14